Chapter 2

# Application of Open-die Warm Extrusion Technique in Spur Gear Manufacturing

Wei Wang and Jun Zhao

Additional information is available at the end of the chapter

http://dx.doi.org/10.5772/intechopen.68503

**Abstract**

The open-die warm extrusion technique is recommended for spur gear manufacturing. This forming technique is systematically researched by using numerical simulation analysis and physical experiments. The lubricating condition, entrance angle, and initial blank size are determined as the crucial factors on the forming quality. The influence of each factor on this technology is fully understood and ascertained. The reasons for causing the forming defect in insufficient sections are analyzed and the die structure and extrusion speed are optimized by using the response surface method (RSM) for defects control and improving the forming quality. Furthermore, the improved process, "Variable Contour Two-Step Warm Extrusion," is presented in order to obtain good forming results in a poor lubricating condition.

**Keywords:** open die, warm extrusion, spur gear

## 1. Introduction

Traditional manufacturing method of spur gears is tooth machining from a round billet, which has the disadvantage of low material utilization. Also, the comprehensive mechanical performance is weakened as a result of metal fibers having been cut off. With the growing severity of energy crisis and environment problems, a new technology is urgently desired to be developed to replace the traditional manufacturing method. Spur gears manufacturing by forming technique can effectively overcome the above shortcomings. This is also beneficial for light weight spur gears because of retained metal fibers and increased power density [1]. Forging is one of the forming technologies first recommended for spur gears manufacturing. Closed-die forging [2, 3], floating die design [4–6], divided flow method [7, 8], and a series of improved technologies have been developed [9–12]. Throughout its development history, a

key constraint of the spur gear forging is the contradictory relationship between the forming load and the forming precision.

Compared with the spur gear forging process, open-die extrusion has the advantage of lower forming load, which has the great significance to prolong die life [13, 14]. Pinions and splined shafts with small modules have been manufactured by extrusion technique [15, 16]. Open-die warm extrusion technique is a combination of the warm forming and the extrusion process, which has a series of obvious advantages: (1) compared with hot forming, this technology can effectively reduce the metal oxidation and decarburization and prevent overheating, overburning, and grain growth, (2) compared with cold forming, this technology can manufacture large module gears and avoid material cracking, and (3) compared with gear forging process, this technology needs smaller forming load so that it can overcome the premature die failure [17, 18].

Based on the advantages of the open-die warm extrusion, it has been developed by authors to manufacture spur gears [19, 20]. A comprehensive study of the open-die warm extrusion process of spur gears is carried out. The influence factors of this technology are fully explored. The RSM is adopted to control the forming defects and improve the forming quality. In addition, an improved process is presented.

## 2. Process model and forming principle

### 2.1. Process model

The process model of open-die warm extrusion of spur gear is illustrated in **Figure 1**. The punch is designed as a gear-like structure in order to avoid a big burr using a round punch or a big forming force using a whole tooth punch. The die includes an entrance section and a forming section. The entrance section has a correlative entrance angle ($\theta$) and height ($h$) and the forming section has toothed contour. High-precision gears need grinding or honing, so the forming section has a contour offset $\Delta$ (0.30 mm) as machining allowance. In the extrusion

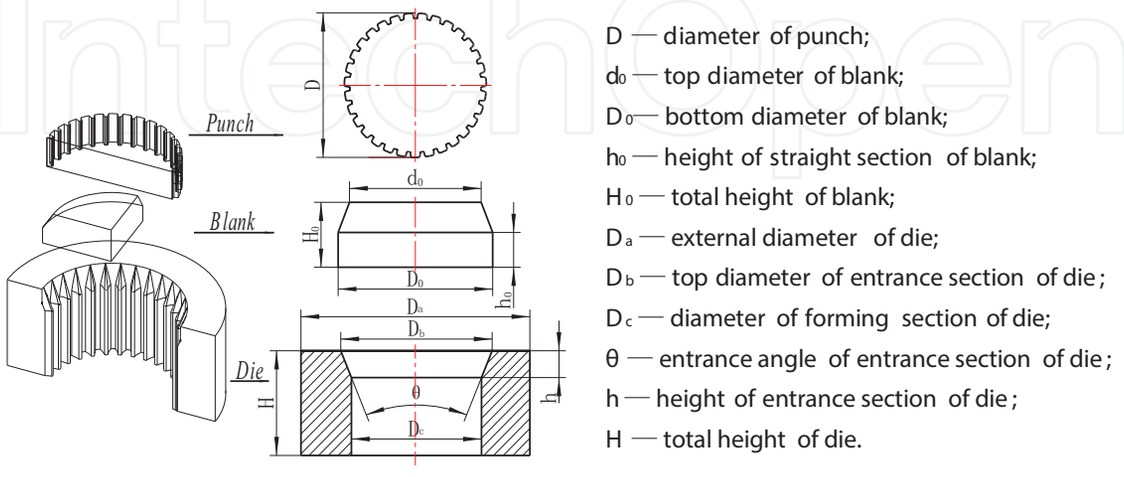


**Figure 1.** The process model of open-die warm extrusion of spur gear.

forming process, besides the lateral extrusion for gear teeth forming, backward extrusion caused by friction occurs simultaneously, so the initial blank is chamfered in its head.

### 2.2. Forming principle

The forming principle and load-stroke curve are shown in **Figure 2**. It consists of three stages. In stage OA, the bottom of the blank is divided by the entrance section. In stage AB, the bottom of the blank is formed into gear tooth shape, and the blank is divided continually. In stage BC, the blank entirely gets into the forming section and the gear teeth go through truing until the blank breaks away from the die.

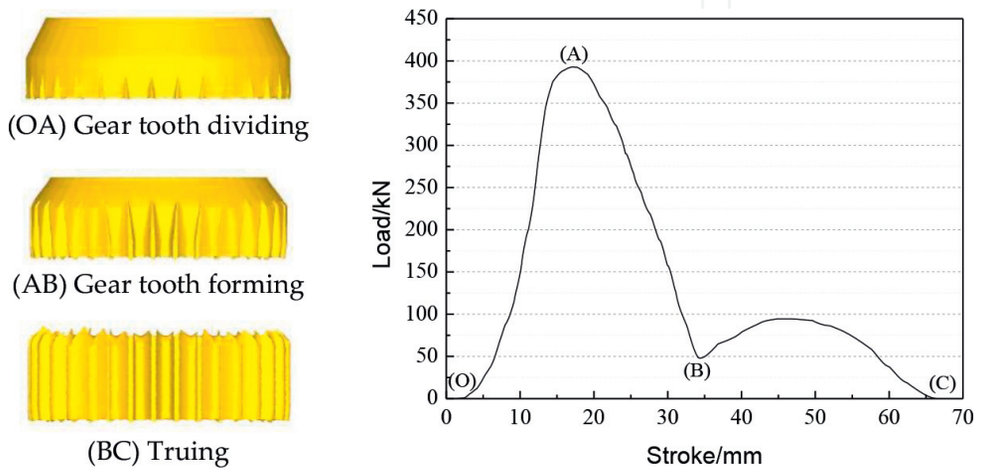


**Figure 2.** Forming principle and load-stroke curve.

## 3. Influence factors analysis

Based on DEFORM-3D, a commercial finite element (FE) software with rigid plastic model and shear friction model ($\tau_f = mk$), the FE model of the open-die warm extrusion is established to explore the influence factors on the forming quality. The FE model is shown in **Figure 3**. The

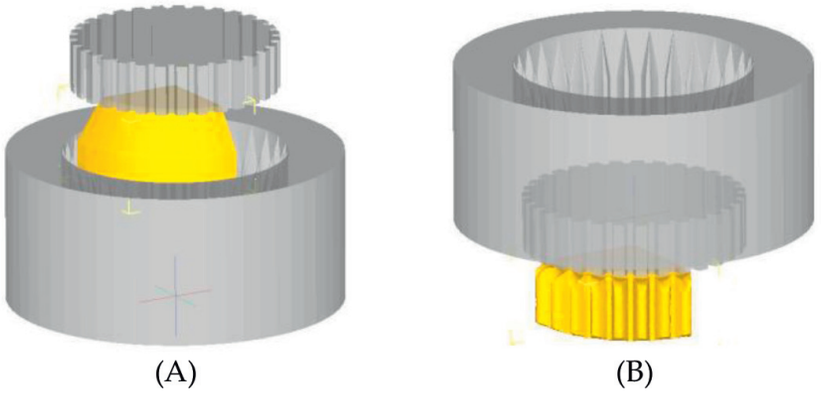


**Figure 3.** The FE model. (A) Before forming; (B) after forming.

detailed parameters of the FE model are listed in **Table 1**. Eight teeth are chosen in the FE model for better clarity. The element type is tetrahedron, element number is 50,000, node number is 11,249, and minimum edge length is 0.4617 mm.

The foreseeable factors' influence on the forming quality include initial blank size, entrance angle of die, friction factor, extrusion speed, and forming temperature. Four levels are set up for each factor (as listed in **Table 2**) to constitute the $L_{16}(4^5)$ orthogonal array. It should be noted that the initial blank size is determined by the equal volume principle and the height of the straight section ($h_0$) is determined as a variable. The orthogonal array and experimental results are listed in **Table 3**.

Through the orthogonal experiment, the lubricating condition, entrance angle, and initial blank size are determined as the crucial factors on the forming quality. However, the experimental results in the orthogonal array suggest different forming defects such as insufficient section, material accumulation, and defect section. So, it is unable to make quantitative analysis. Therefore, the quantitative analysis of each crucial factor is investigated by using the single factor experiment.

### 3.1. Lubricating condition

Lubricating condition is the most significant factor influence on the forming quality. When the friction factor is large, the insufficient section will be formed at the bottom of workpiece, and the flashes will be formed at the top of workpiece as shown in **Figure 4A**. This is due to the metal material backward flows seriously caused by large friction. The influence of the

| Parameter | Tooth number | Modules | Tooth thickness | Material | Die temperature | $\lambda_1$ | $\lambda_2$ |
|---|---|---|---|---|---|---|---|
| Value | 31 | 2 | 20 mm | $20Cr_2Ni_4A$ | 473.15K | 5N/(s·mm·C) | 0.02N/(s·mm·C) |

$\lambda_1$ is the heat transfer coefficient between the blank and the die.
$\lambda_2$ is the convection coefficient to environment.

**Table 1.** Detailed parameters of the FE model.

| Factor | Level | | | |
|---|---|---|---|---|
| | **1** | **2** | **3** | **4** |
| Straight section height $h_0$ (mm) | 5 | 8 | 10 | 15 |
| Entrance angle $\theta$ (°) | 20 | 36 | 52 | 78 |
| Forming temperature (K) | 973.15 | 1073.15 | 1173.15 | 1273.15 |
| Friction factor | 0.2 | 0.3 | 0.5 | 0.7 |
| Extrusion speed $V$ (mm·s$^{-1}$) | 10 | 20 | 30 | 40 |

**Table 2.** Factors and levels.

| Scheme | Straight section height $h_0$ (mm) | Entrance angle $\theta$ (°) | Forming temperature (K) | Friction factor | Extrusion speed (mm·s$^{-1}$) | Experimental result |
|---|---|---|---|---|---|---|
| 1 | 5 | 20 | 973.15 | 0.2 | 10 | Defect section |
| 2 | 5 | 36 | 1073.15 | 0.3 | 20 | Defect section |
| 3 | 5 | 52 | 1173.15 | 0.5 | 30 | Insufficient section |
| 4 | 5 | 78 | 1273.15 | 0.7 | 40 | Insufficient section |
| 5 | 8 | 20 | 1073.15 | 0.5 | 40 | Defect section |
| 6 | 8 | 36 | 973.15 | 0.7 | 30 | Insufficient section |
| 7 | 8 | 52 | 1273.15 | 0.2 | 20 | Defect section |
| 8 | 8 | 78 | 1173.15 | 0.3 | 10 | Material accumulation |
| 9 | 10 | 20 | 1173.15 | 0.7 | 20 | Insufficient section |
| 10 | 10 | 36 | 1273.15 | 0.5 | 10 | Insufficient section |
| 11 | 10 | 52 | 973.15 | 0.3 | 40 | Defect section |
| 12 | 10 | 78 | 1073.15 | 0.2 | 30 | Material accumulation |
| 13 | 15 | 20 | 1273.15 | 0.3 | 30 | Insufficient section |
| 14 | 15 | 36 | 1173.15 | 0.2 | 40 | Insufficient section |
| 15 | 15 | 52 | 1073.15 | 0.7 | 10 | Material accumulation |
| 16 | 15 | 78 | 973.15 | 0.5 | 20 | Material accumulation |

**Table 3.** $L_{16}(4^5)$ orthogonal array and experimental results.

lubricating condition on maximum forming load and the height of insufficient section are shown in **Figure 4B**. The friction factor is set up from 0.2 to 0.5 at an interval of 0.1, with the fixed parameters: entrance angle at 36°, height of straight section at 10 mm, forming temperature at 1073.15 K, and extrusion speed at 10 mm·s$^{-1}$. It indicates a better lubricating condition with a smaller height of insufficient section and a smaller forming load. It should be noted that

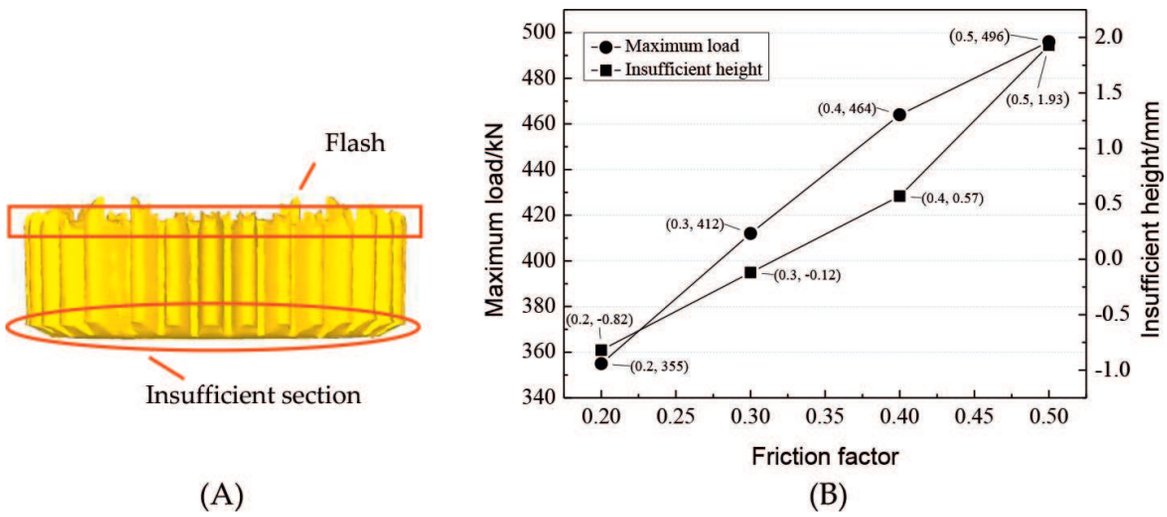


**Figure 4.** Effects of lubricating condition. (A) Forming result in poor lubricating condition; (B) influence of lubricating condition.

when the friction factor is 0.2, the height of the insufficient section presents a negative value (−0.82 mm). This is because the passageway of die is progressively diminishing. When the lubricating condition is very good, the blank will occur forward extrusion in the gear tooth dividing stage. So the addendum is elongated along the extrusion direction.

### 3.2. Entrance angle

Entrance angle of die is the second significant factor. The blank cannot be divided sufficiently when the entrance angle is too large, which will lead to the materials accumulation in the gear tooth-forming stage, as shown in **Figure 5A**. The influence of the entrance angle on the height of the defect section in a good lubrication (friction factor 0.3) condition and the height of the insufficient section in a poor lubrication (friction factor 0.7) condition is shown in **Figure 5B**. An exhibition of the defect section is shown in **Figure 7A**. The entrance angle is set up at 20, 36, and 52°, with the fixed parameters: friction factor at 0.3, height of straight section at 10 mm, forming temperature at 1073.15 K, and extrusion speed at 10 $mm \cdot s^{-1}$. It reveals that both heights of the defect section and the insufficient section decrease with the increase of the entrance angle on the premise of no materials accumulation. But it should be noted that the larger entrance angle leads to the increase of forming load in the gear tooth dividing stage as shown in **Figure 6**. When the entrance angle is 52°, the forming load is markedly increased that is harmful to die life. When the entrance angle is 36°, the forming load of the truing stage is higher than others (the dotted area in **Figure 6**). It means that the contact between the work-piece and the die is better, namely, the gear tooth has a better forming result. So, 36° is a more reasonable choice for the entrance angle.

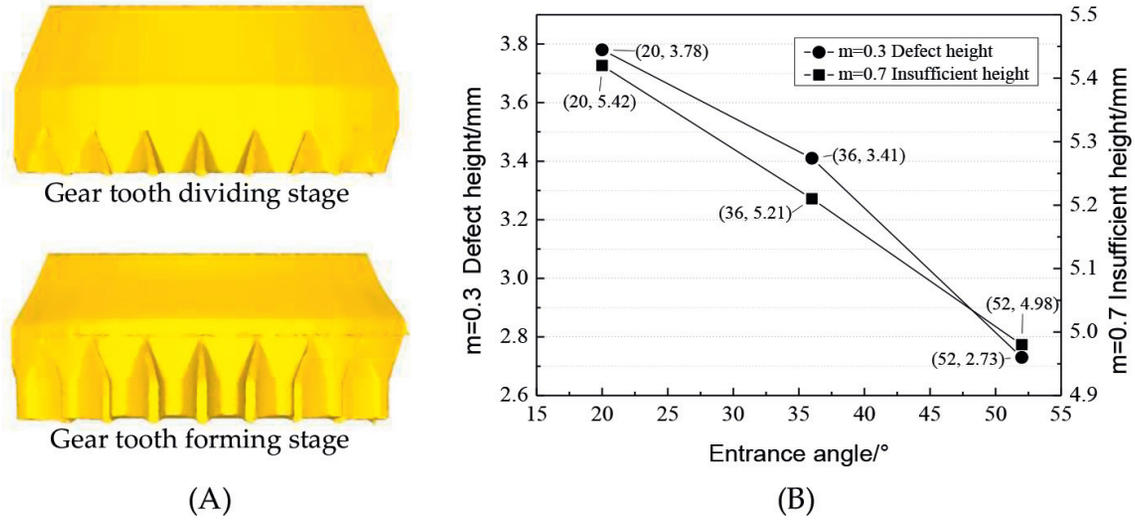


**Figure 5.** Effects of the entrance angle. (A) Material accumulation when entrance angle is 78°; (B) influence of entrance angle.

### 3.3. Initial blank size

If process parameters are set up unreasonably, defect sections will be generated at the top of the blank. The defect section will be aggravated if the straight section of the blank is too short (**Figure 7A**). Conversely, if the straight section is too long, the burr will be formed by

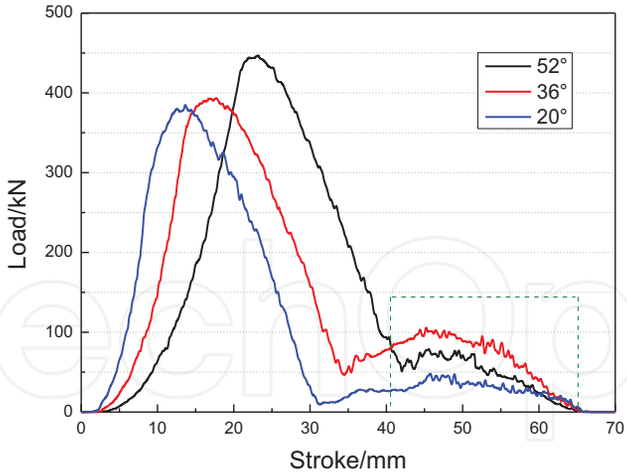


**Figure 6.** Effects of the entrance angle on forming load.

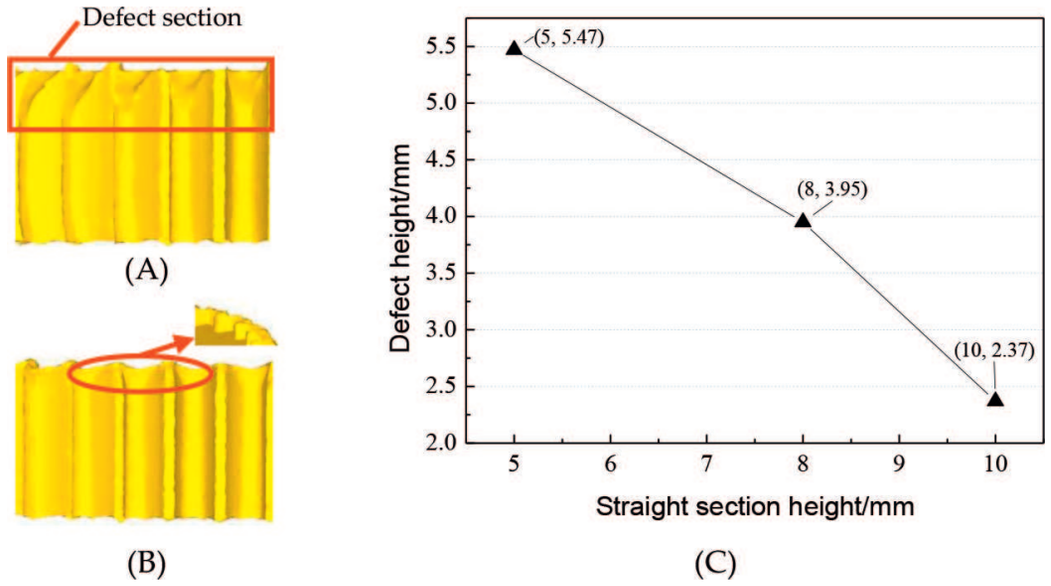


**Figure 7.** Effects of initial blank size. (A) Straight section 5 mm; (B) Straight section 15 mm; (C) Influence of straight section height.

non-filling materials (**Figure 7B**). The influence of the initial blank size on the height of the defect section is shown in **Figure 7C**. The height of the straight section is set up at 5, 8, 10, and 15 mm, with the fixed parameters: entrance angle at 36°, friction factor at 0.3, forming temperature at 1073.15 K, and extrusion speed at 10 mm·s$^{-1}$. It is observed that the longer straight section results in the shorter defect section and better forming quality. Even so, the burr should be avoided by selecting a reasonable initial blank size.

### 3.4. Preliminary experiment

Through the above analysis, the optimized parameters of three crucial factors are ascertained as friction factor 0.3, entrance angle 36°, and straight section 10 mm. The forming temperature

is set as 1073.15 K. Because of the temperature fluctuation, the experimental heating temperature is limited to 1048.15 ± 25 K. The reason is that the plasticity of $20Cr_2Ni_4A$ steel is good and the oxidation is not serious in this temperature. According to the parameters of experimental equipment, the extrusion speed is chosen as 10 $mm \cdot s^{-1}$. Based on the above parameters, the experimental schemes are selected. The experimental equipment is YA-315T hydraulic press and the heating equipment is GP-60 ultra-audio-frequency induction heater. Preheating temperature on the die is 473.15–523.15 K. The experimental material is $20Cr_2Ni_4A$ steel. Oil-based graphite, water-based graphite, and lead oxide are, respectively, chosen as lubricants. **Figure 8** shows the initial blank, the die, and the experimental samples. Unfortunately, all of the experimental schemes do not achieve the desired forming results. The forming effects are similar to the finite element simulation results when the friction factor is 0.6. The insufficient section generates at the bottom of the workpiece, and there still are underfilling teeth.

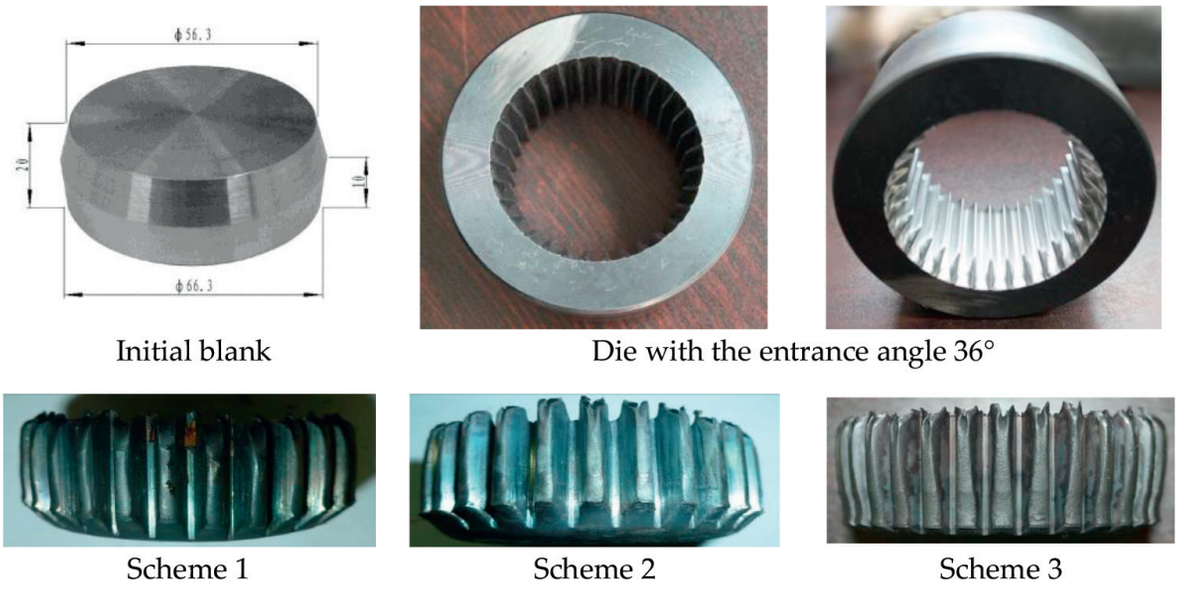


**Figure 8.** Initial blank, die, and experimental samples.

## 4. Optimum die design

Through the preliminary experiment studies, it is found that a good lubricating condition is extremely difficult to achieve caused by the complex contact surfaces between the blank and the die. A pursuit of good lubricating condition will certainly put forward rigorous demands on the die surface quality and the selection of lubricants, which will result in an increased production cost. In addition, the lubricating condition will certainly become worse with continued production. So, it is important to study how the good-quality spur gears can also be formed in a poor lubricating condition.

### 4.1. Defect cause analysis

An important reason for insufficient section is the deterioration of lubricating condition. **Figure 4B** shows the influence of the lubricating condition on the height of insufficient section. The insufficient

http://dx.doi.org/10.5772/intechopen.68503

section almost disappears in good lubricating condition. With the deterioration of the lubricating condition, the height of insufficient section tends to increase. **Figure 9** shows the velocity fields for two cases. One workpiece with insufficient section is shown in **Figure 9A** and another workpiece without defect is shown in **Figure 9B**. It can be seen from the figures that the velocity field is unbalanced in the case of the insufficient section and the generating area is located in the transition zone from entrance section to forming section. After the workpiece passes through the transition zone into the forming section, the velocity field tends to be more balanced. So, the die structure of transition zone is also an important factor that causes the insufficient section.

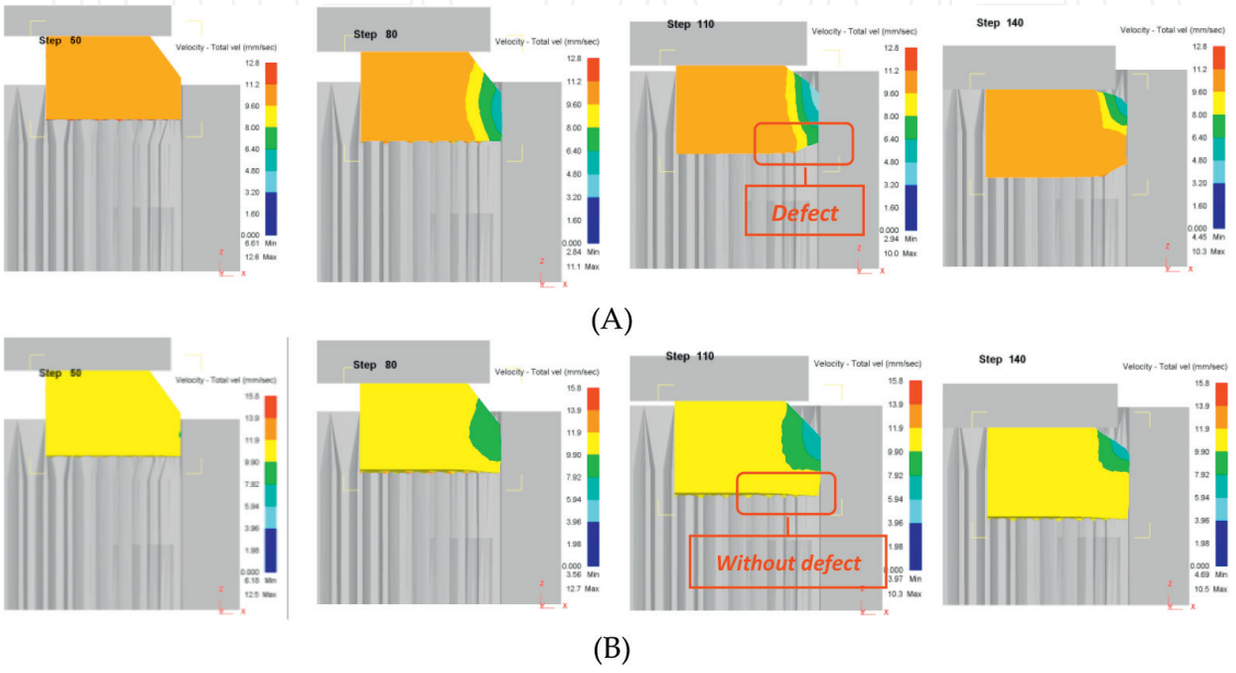


**Figure 9.** Velocity field of workpiece during open-die warm extrusion. (A) Workpiece with insufficient section; (B) workpiece without insufficient section.

Through the above analysis, the main reason causing the insufficient section of gear face is the unbalanced velocity field during the extrusion process—lubricating condition and die structure being two decisive factors. (1) Lubricating condition: the friction between the workpiece and the die increases with the deterioration of lubricating condition, and the reverse axial strain dominates the deformation results in the insufficient section. (2) Die structure: the bottom of the blank is divided by the entrance section. Then, the material flows into the forming section to form gear tooth. In this step, the passageway is progressively diminishing. If the metal flow velocity is under serious disequilibrium, the hard-deformation zone will be generated, resulting in the insufficient section. So, improvement of the lubricating condition and adjustment of the die structure are two corresponding control strategies. The improvement of the lubricating condition is difficult and costly. Therefore, in this chapter, the method is focused on the optimized design of the die structure for defects control and the improvement of forming quality.

### 4.2. Design variables

*Profile variable ratio* at the entrance section (*PVR*):

$$PVR = \frac{S_e - S_f}{S_e} \tag{1}$$

where $S_e$ is the axial projection area on the top of the entrance section and $S_f$ is the axial projection area on the bottom of the entrance section (it is also the axial projection area of the forming section). **Figure 10** shows the sketch of *PVR*, which is associated with the contour offset of forming section (Δ), and it decreases with the increase of Δ, as shown in **Figure 11**. So, *PVR* can be indicated by Δ.

*Profile variable rate* at the entrance section (*PVR′*):

$$PVR' = \frac{PVR}{h} \tag{2}$$

where $h$ is the height of the entrance section and is associated with the entrance angle of entrance section ($\theta$), and it decreases with the increase of $\theta$. So, *PVR′* increases with the increase of $\theta$, and it can be indicated by $\theta$.

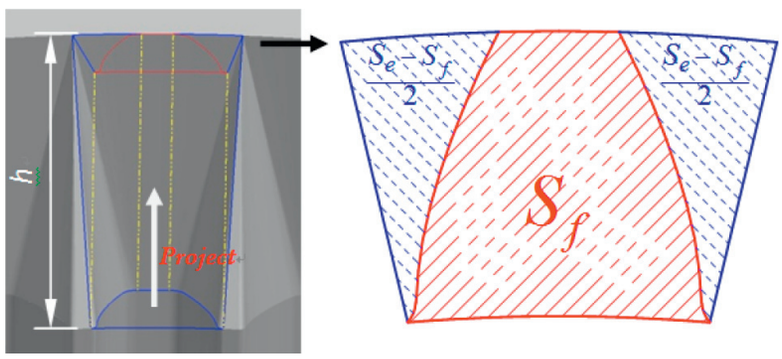


**Figure 10.** Sketch of *PVR*.

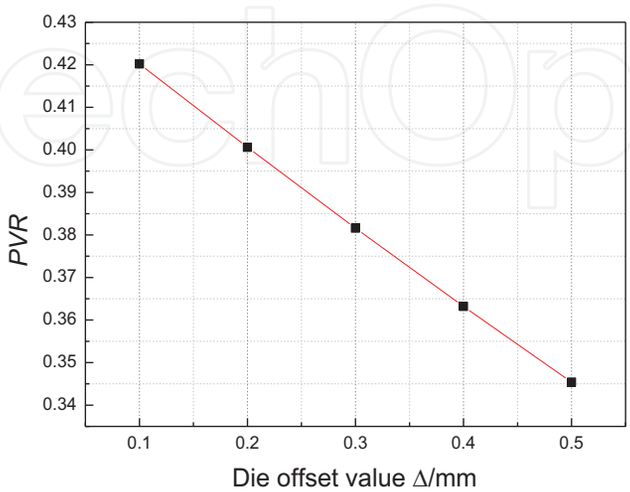


**Figure 11.** Relationship between *PVR* and Δ.

*Extrusion speed* ($V$):

The extrusion speed is also an important influence factor on metal flow velocity. So, $V$ is set as the third design variable. According to the equipment capacity, the extrusion speed ranges from 10 to 50 mm/s.

### 4.3. Objective function

The evaluation index of forming usually includes forming load, forming quality, die life, etc. The forming load of warm extrusion is much less than forging; the common hot work tool steel can meet all performance requirements for warm extrusion die. So, forming quality is the only important factor in evaluation index for objective functions.

The evaluation index of the height of insufficient section is

$$Min : f_1 = \frac{H_s}{H_g} \tag{3}$$

where $H_s$ is the height of insufficient section and $H_g$ is the total height of workpiece.

The evaluation index of filling quality of gear tooth is

$$Min : f_2 = 1 - \frac{R_g}{R_d} \tag{4}$$

where $R_g$ is the radius of the addendum circle of the formed gear and $R_d$ is the radius of addendum of toothed die. $R_g/R_d = \lambda$ and $\lambda$ can be called tooth filling coefficient.

### 4.4. Experimental design and results

This optimized design is a multi-objective optimization problem with three variables and two objectives. The objective functions are optimized by using the response surface method (RSM), and the levels of design variables and process parameters are listed in **Table 4**. The result of the preliminary experiment is similar to the result of numerical simulation when the friction factor is 0.6. So, the friction factor is set as 0.6. Fifteen experimental schemes are established by using central composite design with three factors and three levels. The experimental schemes and results are listed in **Table 5**. The prediction models of $f_1$ and $f_2$ are respectively established by using the complete second-order model:

| Design variable | Δ (mm) (PVR) | θ (°) (PVR′) | V (mm/s) | Forming temperature (K) | Friction factor |
|---|---|---|---|---|---|
| Low level | 0.1 (PVR 0.4202) | 20 (PVR′ 0.0165) | 10 | 1073.15 | 0.6 |
| High level | 0.5 (PVR 0.3454) | 70 (PVR′ 0.0654) | 50 | | |
| Center level | 0.3 (PVR 0.3816) | 45 (PVR′ 0.0318) | 30 | | |

**Table 4.** Design variables and process parameters.

| Scheme | Δ (mm) (*PVR*) | *θ* (°) (*PVR′*) | *V* (mm/s) | $f_1$ | $f_2$ |
|---|---|---|---|---|---|
| 1 | 0.3 (*PVR* 0.3816) | 45 (*PVR′* 0.0351) | 50 | 0.163636 | 0.003580 |
| 2 | 0.1 (*PVR* 0.4202) | 20 (*PVR′* 0.0165) | 10 | 0.433333 | 0.002039 |
| 3 | 0.1 (*PVR* 0.4202) | 20 (*PVR′* 0.0165) | 50 | 0.213333 | 0.000914 |
| 4 | 0.3 (*PVR* 0.3816) | 45 (*PVR′* 0.0351) | 30 | 0.150909 | 0.002196 |
| 5 | 0.5 (*PVR* 0.3454) | 45 (*PVR′* 0.0318) | 30 | 0.047273 | 0.000897 |
| 6 | 0.3 (*PVR* 0.3816) | 70 (*PVR′* 0.0594) | 30 | 0.184848 | 0.003966 |
| 7 | 0.1 (*PVR* 0.4202) | 45 (*PVR′* 0.0387) | 30 | 0.262424 | 0.001560 |
| 8 | 0.1 (*PVR* 0.4202) | 70 (*PVR′* 0.0654) | 10 | 0.456364 | 0.013768 |
| 9 | 0.5 (*PVR* 0.3454) | 20 (*PVR′* 0.0135) | 50 | 0.134182 | 0.001103 |
| 10 | 0.5 (*PVR* 0.3454) | 70 (*PVR′* 0.0537) | 50 | 0.129091 | 0.003332 |
| 11 | 0.5 (*PVR* 0.3454) | 20 (*PVR′* 0.0135) | 10 | 0.111515 | 0.001101 |
| 12 | 0.1 (*PVR* 0.4202) | 70 (*PVR′* 0.0654) | 50 | 0.292727 | 0.008369 |
| 13 | 0.3 (*PVR* 0.3816) | 20 (*PVR′* 0.0150) | 30 | 0.173333 | 0.000624 |
| 14 | 0.3 (*PVR* 0.3816) | 45 (*PVR′* 0.0351) | 10 | 0.229697 | 0.003399 |
| 15 | 0.5 (*PVR* 0.3454) | 70 (*PVR′* 0.0537) | 10 | 0.059394 | 0.002732 |

**Table 5.** Experimental schemes and results.

$$\begin{aligned} f_1 = {} & 0.68869 - 0.91381\Delta - 3.40655 \times 10^{-3}\alpha - 0.014273V \\ & - 3.99091 \times 10^{-3}\Delta\alpha + 0.014875\Delta V + 2.58485 \times 10^{-5}\alpha V \\ & + 0.097980\Delta^2 + 4.50586 \times 10^{-5}\alpha^2 + 1.14343 \times 10^{-4}V^2 \end{aligned} \tag{5}$$

$$\begin{aligned} f_2 = {} & 2.35514 \times 10^{-3} + 6.00054 \times 10^{-3}\Delta + 1.34600 \times 10^{-4}\alpha \\ & - 3.51418 \times 10^{-4}V - 3.83087 \times 10^{-4}\Delta\alpha + 2.22694 \times 10^{-4}\Delta V \\ & - 9.18613 \times 10^{-7}\alpha V - 6.97470 \times 10^{-3}\Delta^2 + 1.26034 \times 10^{-6}\alpha^2 \\ & + 4.95393 \times 10^{-6}V^2 \end{aligned} \tag{6}$$

Significance of each prediction model is analyzed by using analysis of variance; the results are respectively listed in **Tables 6** and **7**. The *R*-squared of $f_1$ and $f_2$, respectively, are 0.998569 and 0.930357; the Adj *R*-squared, respectively, are 0.995995 and 0.804999 and the *P*-values respectively are < 0.0001 and 0.0200. These data indicate that the response value is extremely significant. The prediction models both have good accuracy.

### 4.5. Response surface analysis

The 3D response surface plots and contour plots of $f_1$ are shown in **Figures 12–14**. The response $f_1$ decreases with the decrease of *PVR* (increase of Δ); it first decreases and then increases with the increase of *PVR′* (*θ*); similarly, with the increase of *V*, the response $f_1$ first decreases and then increases.

| Source | Sum of squares | df | Mean square | *F* value | *P*-value |
|---|---|---|---|---|---|
| | | | | | Prob > *F* |
| Model | 0.198278 | 9 | 0.022031 | 387.805855 | < 0.0001 |
| $\Delta$ | 0.138469 | 1 | 0.138469 | 2437.441605 | < 0.0001 |
| $\alpha$ | 0.000322 | 1 | 0.000322 | 5.664562 | 0.0632 |
| $V$ | 0.012769 | 1 | 0.012769 | 224.765496 | < 0.0001 |
| $\Delta\alpha$ | 0.003185 | 1 | 0.003185 | 56.073317 | 0.0007 |
| $\Delta V$ | 0.028322 | 1 | 0.028322 | 498.547451 | < 0.0001 |
| $\alpha V$ | 0.001336 | 1 | 0.001336 | 23.522461 | 0.0047 |
| $\Delta^2$ | 0.000039 | 1 | 0.000039 | 0.695264 | 0.4424 |
| $\alpha^2$ | 0.002039 | 1 | 0.002039 | 35.898160 | 0.0019 |
| $V^2$ | 0.005379 | 1 | 0.005379 | 94.688992 | 0.0002 |
| Residual | 0.000284 | 5 | 0.000057 | | |

Standard deviation: 0.007537, *R*-squared: 0.998569. press: 0.002699, and Adj *R*-squared: 0.995995.

**Table 6.** Variance analysis of prediction model $f_1$.

| Source | Sum of squares | df | Mean square | *F* value | *P*-value |
|---|---|---|---|---|---|
| | | | | | Prob > *F* |
| Model | 0.000158 | 9 | 0.000018 | 7.421595 | 0.0200 |
| $\Delta$ | 0.000031 | 1 | 0.000031 | 12.891600 | 0.0157 |
| $\alpha$ | 0.000069 | 1 | 0.000069 | 29.359567 | 0.0029 |
| $V$ | 0.000003 | 1 | 0.000003 | 1.390494 | 0.2914 |
| $\Delta\alpha$ | 0.000029 | 1 | 0.000029 | 12.376901 | 0.0170 |
| $\Delta V$ | 0.000006 | 1 | 0.000006 | 2.676781 | 0.1627 |
| $\alpha V$ | 0.000002 | 1 | 0.000002 | 0.711676 | 0.4374 |
| $\Delta^2$ | 0.000001 | 1 | 0.0000001 | 0.084398 | 0.7831 |
| $\alpha^2$ | 0.000002 | 1 | 0.000002 | 0.672817 | 0.4494 |
| $V^2$ | 0.000010 | 1 | 0.000010 | 4.257755 | 0.0940 |
| Residual | 0.000012 | 5 | 0.000002 | | |

Standard deviation: 0.001540, *R*-squared: 0.930357, press: 0.000149, and Adj *R*-squared: 0.804999.

**Table 7.** Variance analysis of prediction model $f_2$.

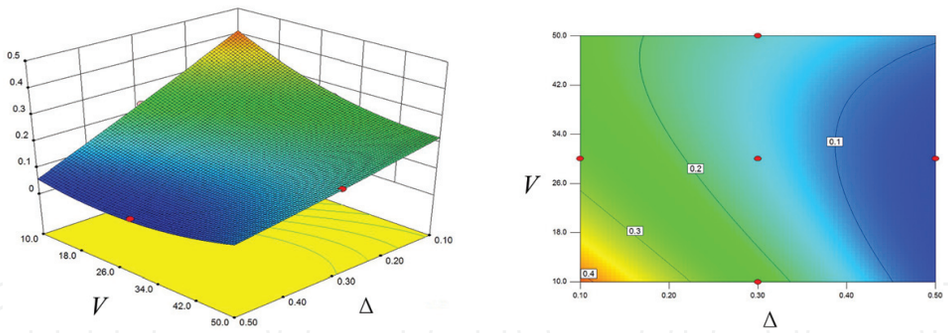


**Figure 12.** Interaction between $V$ and $\Delta$ on $f_1$ with $\theta = 45°$.

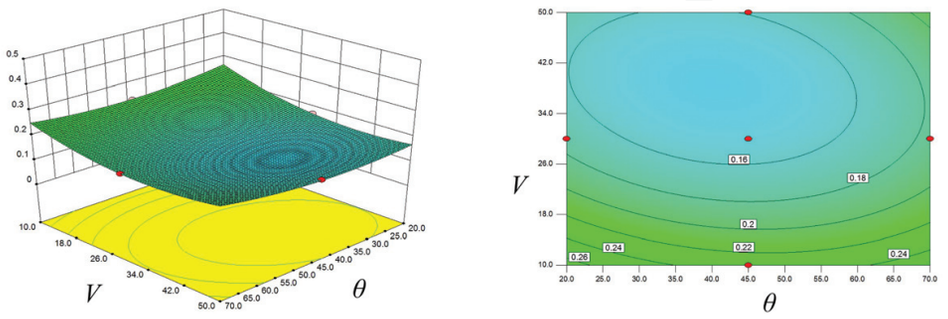


**Figure 13.** Interaction between $V$ and $\theta$ on $f_1$ with $\Delta = 0.3$ mm.

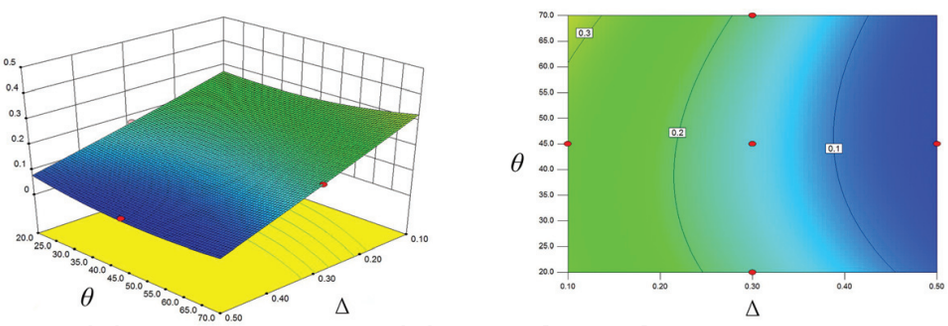


**Figure 14.** Interaction between $\theta$ and $\Delta$ on $f_1$ with $V = 30$ mm/s.

Reason analysis: (1) with the decrease of $PVR$ (increase of $\Delta$), the channel of the metal axial flow is enlarged; the variable ratio from the entrance section to the forming section is reduced; the axial flow resistance of the metal is reduced, and so the height of insufficient section is decreased. (2) When the extrusion speed $V$ is slower, the temperature drop of workpiece is quicker, the plasticity of metal is decreased, and then the axial flow of metal is weakened. With the increase of the extrusion speed, the metal deformation energy cannot be timely released, which is conducive to metal flow. However, the extrusion speed continues to increase, the blank does not have enough time for tooth graduation, and this results in the increase of the height of insufficient section. (3) If the entrance angle $\theta$ ($PVR'$) is too small, namely, the height of the entrance section ($h$) is too high, although the workpiece is fully graduated, the temperature of the workpiece is significantly cooled before into the forming section, and then the plasticity of metal

http://dx.doi.org/10.5772/intechopen.68503

is decreased, resulting in the height of higher insufficient section. With the increase of $\theta$, this issue is alleviated; the height of insufficient section is decreased. If the entrance angle ($\theta$) is too large, the workpiece cannot be fully graduated, and the hard-deformation zone will be generated from the material accumulation in the forming stage, and then the height of insufficient section is increased. When at high extrusion speeds, the height of insufficient section is increased with the increase of $\theta$, but not decreased, this due to the temperature drop becomes a secondary factor, and the die structure becomes a determining factor.

The 3D response surface plots and contour plots of $f_2$ are shown in **Figures 15–17**. The response $f_2$ decreases with the decrease of $PVR$ (increase of $\Delta$); it increases with the increase of $PVR'$ ($\theta$); it first decreases and then increases with the increase of $V$.

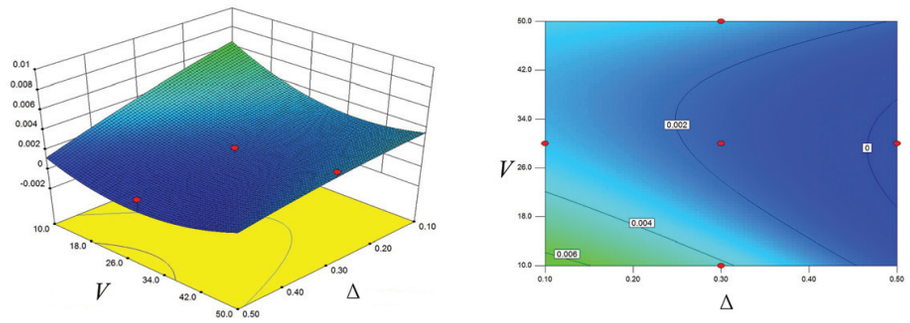


**Figure 15.** Interaction between $V$ and $\Delta$ on $f_2$ with $\theta = 45°$.

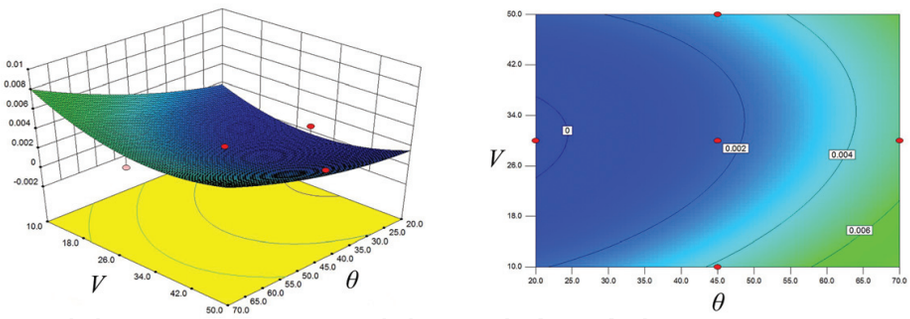


**Figure 16.** Interaction between $V$ and $\theta$ on $f_2$ with $\Delta = 0.3$ mm.

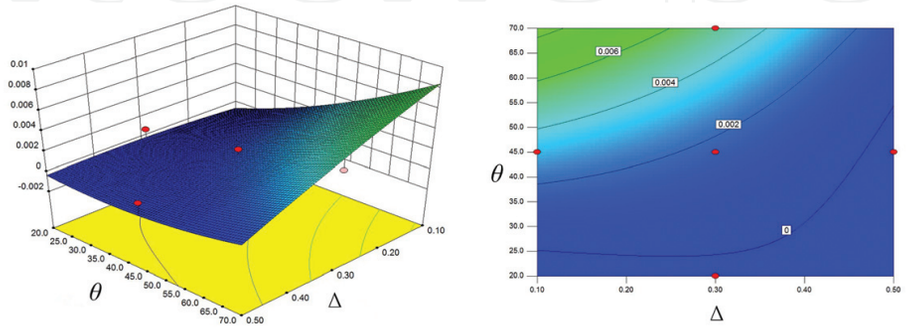


**Figure 17.** Interaction between $\theta$ and $\Delta$ on $f_2$ with $V = 30$ mm/s.

Reason analysis: (1) with the decrease of $PVR$ (increase of $\Delta$), the channel of metal radial flow is enlarged; the radial flow resistance of the metal is reduced, and so filling quality of gear tooth is improved. (2) When the extrusion speed $V$ is slower, the temperature drop of workpiece is quicker. The plasticity of metal is decreased, and then the radial flow of metal is weakened. With the increase of the extrusion speed, the metal deformation energy cannot be timely released, which is conducive to metal radial flow. However, the extrusion speed continues to increase; the radial flow is weakened because the rigid translation of inner zone and axial deformation of outer zone become predominant, so the filling quality of gear tooth becomes poor. This rule is same with the influence of $V$ on response $f_1$. When the extrusion speed is too high, the height of insufficient section is higher and the filling quality of gear tooth is worse. (3) With the increase of $PVR'$ ($\theta$), the height of entrance section ($h$) is decreased. The ability of graduation for the workpiece by the entrance section is decreased; if the workpiece cannot be fully graduated, the filling quality of gear tooth is worse.

### 4.6. Experimental verification

The die structure and extrusion speed are optimized by using the RSM with the goals of decreasing the height of insufficient section and improving the filling quality of gear tooth. The optimal values for each factor are $\Delta = 0.49$ mm ($PVR = 0.3471$), $\theta = 46.02°$ ($PVR' = 0.0327$), and $V = 29.51$ mm/s. The corresponding response values are $f_1 = 0.043854$ and $f_2 = 0.000192$. The theoretical machining allowance of tooth tip, tooth flank, and gear face, respectively, are $\Delta$-$R_d f_2$ (0.477 mm), $\Delta$ (0.490 mm), and $H_g f_1$ (0.877 mm).

The numerical simulations are done by adopting the original and the optimized parameters, respectively. The results are shown in **Figure 18**. The response values and the relative error of the simulated results with the optimal results are listed in **Table 8**. It is observed that the

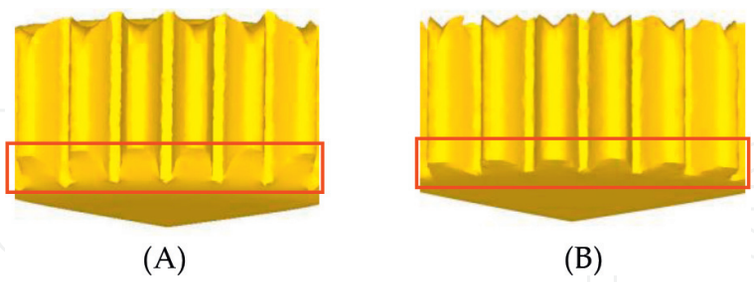


**Figure 18.** Numerical simulation results. (A) Original parameters; (B) optimized parameters.

| Response value | Simulated results with original parameters | Optimized results | Simulated results with optimized parameters | Relative error between simulated and optimized results |
|---|---|---|---|---|
| $f_1$ | 0.237006 | 0.043854 | 0.043939 | 0.1938% |
| $f_2$ | 0.001186 | 0.000192 | 0.000189 | 1.5625% |

**Table 8.** Response values and relative error.

desired optimal result is obtained to decrease the height of insufficient section and improve the filling quality of gear tooth.

The experimental sample is shown in **Figure 19**. The machining allowance is tested by using the 3D coordinate measuring machine. The measuring points of each tooth tip and flank are equispaced at 25 points. As for gear face, each location is measured five times to calculate the mean value. The measurement results are shown in **Figure 20**. Due to the elastic deformation of die and the elastic recovery of workpiece, all the measured values of the tooth flank are with positive deviation.

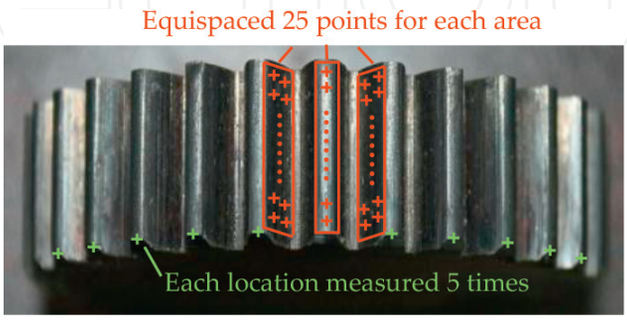


**Figure 19.** Experimental sample.

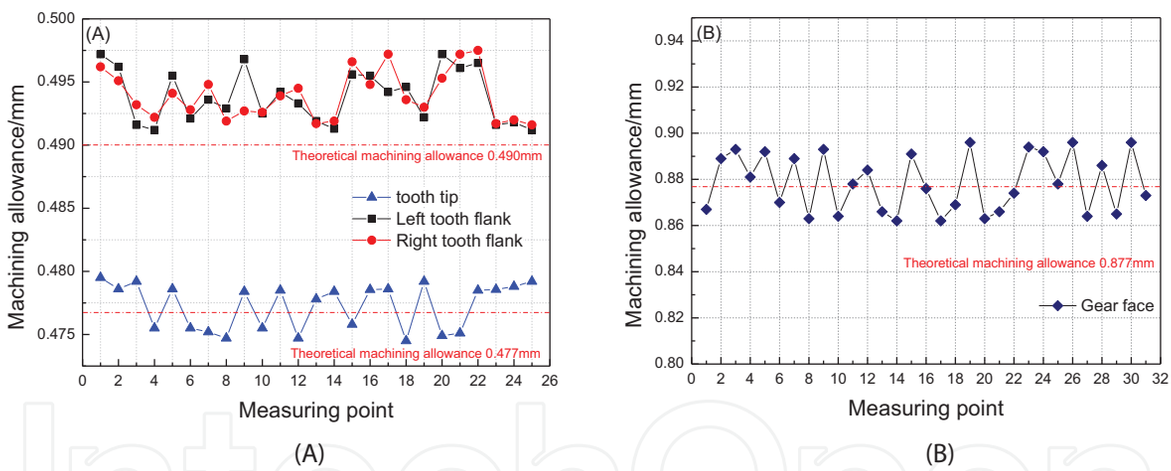


**Figure 20.** Machining allowance measurement. (A) Measurement result of tip and flank; (B) measurement result of gear face.

## 5. Variable contour two-step warm extrusion

Through the die optimum design, the goals of decreasing the height of insufficient section and improving the filling quality of gear tooth are achieved. But the machining allowance of tooth flank rises from the original design of the 0.30 to 0.49 mm. In order to further reduce the machining allowance, "Variable Contour Two-Step Warm Extrusion" is presented. First, pre-extrusion is implemented for a die in which the contour of the forming section is enlarged from the final-toothed contour. The formed spur gear is allowed to have insufficient section after

pre-extrusion. Then, the workpiece is turned around to implement the finish-extrusion by a die with the final-toothed contour for insufficient section compensation and gear tooth sizing. Because the gear tooth has been formed by pre-extrusion, the forming load of finish-extrusion is very small, so the workpiece need not be reheated. **Figure 21A** shows the influence of contour variation on the height of insufficient section when the friction factor is 0.6. It indicates that the height of insufficient section decreases with the increase of contour variation. The insufficient section almost disappears when the contour variation is 0.3 mm. **Figure 21B** shows the simulated results when the contour variation is 0.3 mm.

**Figure 22** shows the experimental sample. The accuracy is tested by using the coordinate measuring machine. Theoretical Computer Aided Design (CAD) model is set as a reference. Twenty-five uniformly distributed spaced points are measured for each gear tooth. The mean error is calculated by $\overline{\delta} = \sum_{i=1}^{25} |\delta_i|/25$. The testing result is shown in **Figure 23A**, and the maximum mean error of single tooth is 15.5 μm. An example of the accuracy testing on one tooth is shown in **Figure 23B**, and the maximum absolute error is 42.7 μm.

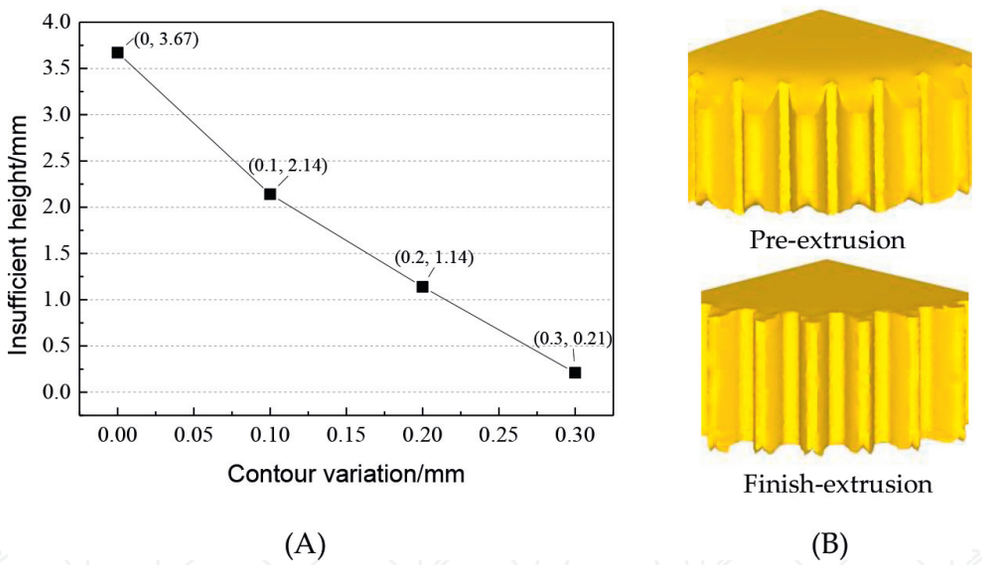


**Figure 21.** Variable contour two-step warm extrusion. (A) Influence of contour variation on forming quality; (B) simulation results.

**Figure 22.** Experimental sample.

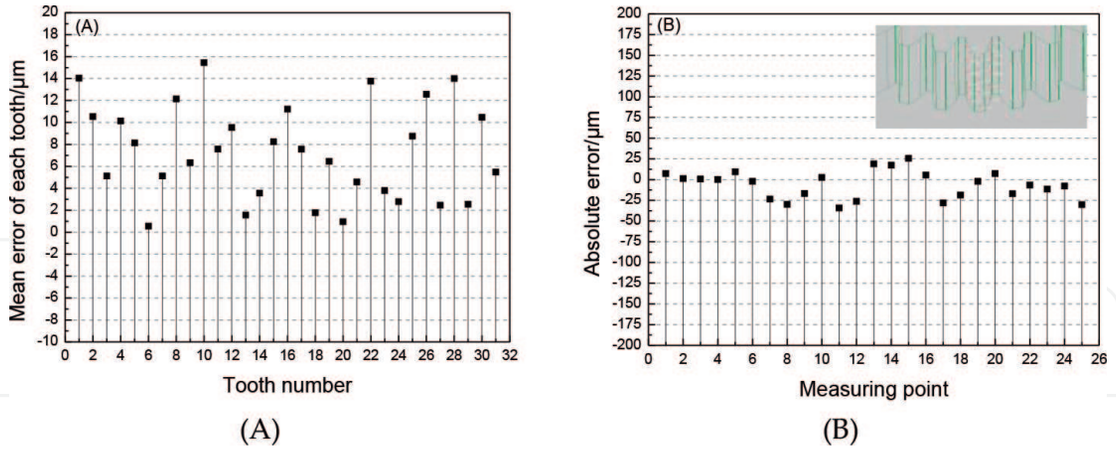


**Figure 23.** Testing results. (A) Mean error of each tooth; (B) an example of accuracy testing.

## 6. Summary

Open-die warm extrusion is developed to replace the traditional manufacturing method of the spur gear. For this technique, lubricating condition, entrance angle, and initial blank size are the crucial factors. Insufficient section will be generated when the lubricating condition is poor. If the entrance angle is too large, material accumulation will occur during the gear tooth forming stage. The defect section will be worse if the straight section is too short.

The main reason for the insufficient section is the unbalanced velocity field. Except for the lubricating condition, the die structure is another decisive factor. The height of insufficient section is decreased with the increase of contour offset. It first decreases and then increases, with the increase of entrance angle. Similarly, with the increase of extrusion speed, it first decreases and then increases. The filling quality of gear tooth improves with the increase of contour offset; it deteriorates with the increase of entrance angle; it first improves and then deteriorates with the increase of extrusion speed.

In order to obtain a good forming result in a poor lubrication, "Variable Contour Two-Step Warm Extrusion" is proposed. Pre-extrusion is for gear teeth forming and finish-extrusion is for insufficient section compensation and tooth sizing. The height of insufficient section decreases with the increase in contour variation. When the contour variation is 0.3 mm, the insufficient section is almost eliminated.

## Author details

Wei Wang and Jun Zhao*

*Address all correspondence to: zhaojun@ysu.edu.cn

Key Laboratory of Advanced Forging & Stamping Technology and Science, Yanshan University, Ministry of Education of China, Qinhuangdao, PR China

## References

[1] Dean TA. The net-shape forming of gears. Materials and Design. 2000;**21**:271-278

[2] Abdul NA, Dean TA. An analysis of the forging of spur gear forms. International Journal of Machine Tool Design and Research. 1986;**26**:113-123

[3] Chitkara NR, Bhutta MA. Near-net shape forging of spur gear forms: an analysis and some experiments. International Journal of Mechanical Sciences. 1996;**38**:891-916

[4] Tuncer C, Dean TA. Die design alternatives for precision forging hollow parts. International Journal of Machine Tools and Manufacture. 1987;**27**:65-76

[5] Tuncer C, Dean TA. Precision forging hollow parts in novel dies. Journal of Mechanical Working Technology. 1988;**16**:39-50

[6] Cai J, Dean TA, Hu ZM. Alternative die designs in net-shape forging of gears. Journal of Materials Processing Technology. 2004;**150**:48-55

[7] Kondo K, Ohga K. Precision cold die forging of a ring gear by divided flow method. International Journal of Machine Tools and Manufacture. 1995;**35**:1105-1113

[8] Choi JC, Choi Y. Precision forging of spur gears with inside relief. International Journal of Machine Tools and Manufacture. 1999;**39**:1575-1588

[9] Wang GC, Zhao GQ, Xia SS, Luan YG. Numerical and experimental study on new cold precision forging technique of spur gears. Transactions of Nonferrous Metals Society of China. 2003;**13**:798-802

[10] Behrens BA, Odening D. Process and tool design for precision forging of geared components. International Journal of Material Forming. 2009;**2**:125-128

[11] Hu CL, Wang KS, Liu QK. Study on a new technological scheme for cold forging of spur gears. Journal of Materials Processing Technology. 2007;**187-188**:600-603

[12] Zuo B, Wang BY, Li Z, Zheng MN, Zhu XX. Design of relief-cavity in closed-precision forging of gears. Journal of Central South University. 2015;**22**:1287-1297

[13] Song JH, Im YT. Determination of a major design parameter for forward extrusion of spur gears. Journal of Manufacturing Science and Engineering. 2004;**126**:255-263

[14] Song JH, Im YT. The applicability of process design system for forward extrusion of spur gears. Journal of Materials Processing Technology. 2007;**184**:411-419

[15] Yuan AF. Cold extrusion of a long trapezium spline and its forming analysis. International Journal of Advanced Manufacturing Technology. 2009;**41**:461-467

[16] Jeong MS, Lee SK, Yun JH, Sung JH, Kim DH, Lee S, Choi TH. Green manufacturing process for helical pinion gear using cold extrusion process. International Journal of Precision Engineering and Manufacturing. 2013;**14**:1007-1011

[17] Niechajowicz A, Tobota A. Warm deformation of carbon steel. Journal of Materials Processing Technology. 2000;**106**:123-130

[18] Li YY, Zhao SD, Fan SQ, Yan GH. Study on the material characteristic and process parameters of the open-die warm extrusion process of spline shaft with 42CrMo steel. Journal of Alloys and Compounds. 2013;**571**:12-20

[19] Wang W, Zhao J, Zhai RX. A forming technology of spur gear by warm extrusion and the defects control. Journal of Manufacturing Processes. 2016;**21**:30-38

[20] Wang W, Zhao J, Zhai RX, Ma R. Variable contour two-step warm extrusion forming of spur gear and the deformation behavior of $20Cr_2Ni_4A$ steel. International Journal of Advanced Manufacturing Technology. 2017;**88**:3163-3173

IntechOpen